Am J Nucl Med Mol Imaging 2022;12(4):122-128
www.ajnmmi.us /ISSN:2160-8407/ajnmmi0145841

Case Report

Multimodal treatment and imaging of primary pulmonary artery sarcoma: a case report

Wenpeng Huang[1*], Yuhan Zhou[2*], Ge Gao[3], Qi Yang[1], Zhao Chen[1], Yongkang Qiu[1], Lele Song[1], Lei Kang[1]

[1]*Department of Nuclear Medicine, Peking University First Hospital, Beijing 100034, PR China;* [2]*Department of Radiology, The First Affiliated Hospital of Zhengzhou University, Zhengzhou 450052, Henan Province, PR China;* [3]*Department of Medical Imaging, Peking University First Hospital, Beijing 100034, PR China.* [*]*Equal contributors.*

Received August 9, 2022; Accepted August 12, 2022; Epub August 20, 2022; Published August 30, 2022

Abstract: Primary pulmonary artery sarcoma (PAS) is a malignant neoplasm of the pulmonary vascular system originating from the intima, with clinical and imaging manifestations similar to those of pulmonary thromboembolism (PTE), and is often misdiagnosed. Spectral CT and PET/CT can clearly show the extent and metastasis of PAS and are valuable in visualizing adjacent structures such as lungs, bronchi, and mediastinum, providing a strong imaging basis for the diagnosis and differentiation of PAS, allowing treatment monitoring and follow-up.

Keywords: Pulmonary artery sarcoma, ^{18}F-FDG, PET/CT, X-ray computed tomography, I-125 seeds

Introduction

Primary pulmonary artery sarcoma (PAS) is a malignant tumor of the pulmonary vascular system originating from the intima and is clinically rare with an incidence of only 0.001% to 0.030% [1, 2]. PAS mostly presents with atypical symptoms such as dyspnea, chest tightness, and chest pain, and it is difficult to be distinguished from pulmonary thromboembolism (PTE). It is more difficult to identify PTE in the early stage, and the diagnosis is mostly confirmed after receiving thrombolytic therapy which is proven to be ineffective followed by further examinations, thus missing the best treatment time and leading to a poor prognosis [3-6].

Here, we report multiple imaging presentation and treatment modalities of a patient with PAS. Although the patient underwent two surgical resections, ^{125}I seeds implantation, and multiple chemotherapies, the patient developed recurrence and metastasis. We discuss the spectral CT and PET/CT imaging features about patients with PAS to improve the level of understanding of this type of disease.

Case presentation

A 55-year-old man who was admitted to the hospital 21 months ago with cough and sputum underwent pulmonary angiography showing a low-density filling defect in the right pulmonary artery trunk and was initially diagnosed with pulmonary embolism. After administration of heparin anticoagulation and fibrinolytic enzyme thrombolytic therapy, the symptoms did not improve. The patient underwent interventional biopsy of the pulmonary artery, and postoperative pathology confirmed a pulmonary artery sarcoma (PAS). After 7 days, the patient underwent pulmonary artery dissection and PAS resection, followed by 6 cycles of chemotherapy with AI regimen (liposomal adriamycin 80 mg plus isocyclophosphamide 2.5 g/3 d) and targeted therapy with "anrotinib". A CT examination was performed 15 months after surgery, which suggested the recurrence of PAS, so that treatment was changed to pablizumab (200 mg) for 9 times. Meanwhile the patient developed hemoptysis and was treated with bronchial interventional embolization. Physical examination showed a tricuspid regurgitant murmur in the pulmonary artery auscultation area and a hyperactive second heart sound (P2 > A2). Laboratory tests showed increased D-dimer at 5.97 mg/mL (normal range 0-0.55 mg/L), fibrinogen at 14.7 g/L (normal range 2-4 g/L), and B-type natriuretic peptide at 6870 ng/mL (normal range 0-100 ng/mL). The patient underwent a chest CT-enhanced examination and showed a hypodense filling

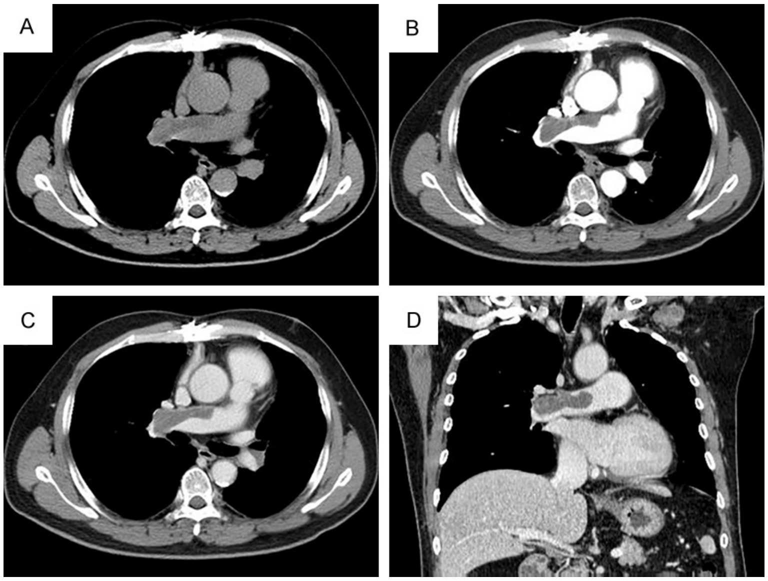

Figure 1. Computed tomography (CT) images of recurrence of pulmonary artery sarcoma after surgery. A. Plain axial image; B. Arterial phase axial image; C. Venous phase axial image; D. Venous phase coronal image.

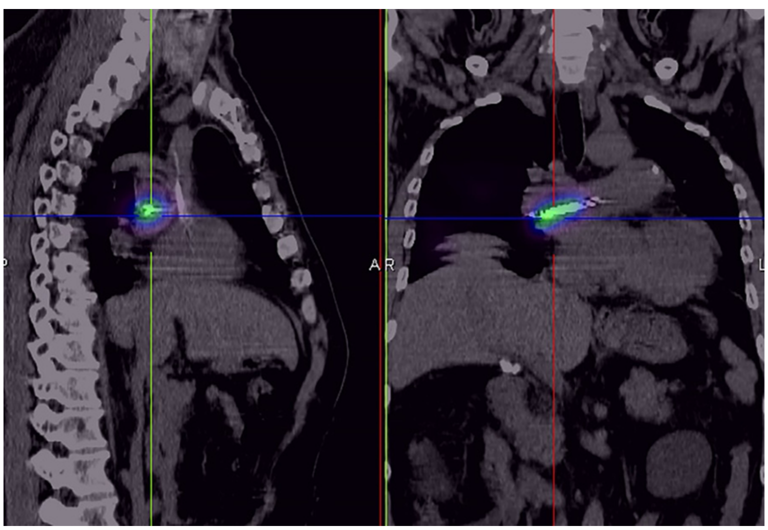

Figure 2. SPECT/CT tomography images after ^{125}I-seeds implantation treatment. A bead-like seeds with metallic density was seen in the right pulmonary artery, with obvious radioactive distribution, indicating well-positioned covering the tumor area.

defect at the bifurcation of the main pulmonary artery trunk and a strip of the right pulmonary artery trunk with a plain CT attenuation value of approximately 38 HU and a mildly enhanced margin after enhancement (**Figure 1**). The patient agreed to receive the treatment of ^{125}I-seeds implantation. SPECT/CT tomography showed a bead-like metallic-dessity seeds in the right pulmonary artery lesion with increased radioactive accumulation, indicating well-positioned seeds covering the tumor area (**Figure 2**). PET/CT examination of the patient 2 months later showed a nodular lesion in the right pulmonary artery wall, with an increased FDG uptake (SUVmax = 7.6), suggesting the recurrence of PAS. Besides, a radiological defect in the right pulmonary artery was shown with a CT attenuation value of approximately 32 HU, suggesting thrombosis (**Figure 3**). 10 days later, the patient developed hemoptysis and a spectral CT-enhanced examination showed the lesion enlargered further (**Figure 4A**). The plain scan electron density (ED) images were obtained after reconstruction by Philips Nebula post-processing workstation and selected the low-density regions of the ascending aorta and right pulmonary artery trunk as regions of interest (ROI > 50 mm^2) with measured values of 104.4% EDW (percentage of electron density relative to water) and 102.8% EDW, respectively (**Figure 4B**, **4C**). The mixed energy and ED fusion map (**Figure 4D**) showed a region of inhomogeneous low electron density in the PAS of the right pulmonary artery trunk, with uniform electron density in the ascending aorta and the rest of the pulmonary artery. According to the high/low radioactive accumulated zone of the right pulmonary artery trunk of PET/CT, compared with the homogeneous mixed energy images, the iodine density (ID) values were measured by selected ROI at 1.76 mg/ml in the PAS zone and 0.03 mg/ml in the thrombus zone, suggesting that the iodine uptake in the PAS zone was significantly higher than in the thrombus zone (**Figure 4E**, **4F**). The slope of the spectral curve was calculated by the formula of $[(HU_{40KeV}-HU_{100KeV})/60]$. The slope of the PAS region was 2.08 whereas the slope of the thrombus region

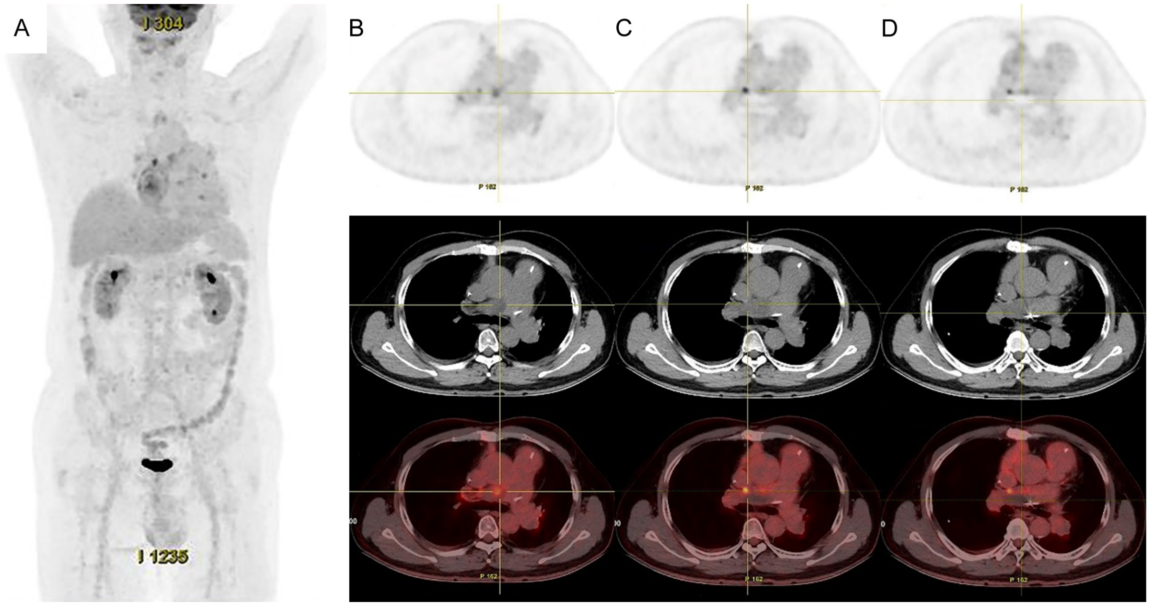

Figure 3. ^{18}F-FDG PET/CT images 2 months after treatment with ^{125}I-seeds implantation. A. The anteroposterior 3-dimensional maximum intensity projection image (MIP) demonstrated a hypermetabolic lesion in the right pulmonary artery trunk while no abnormal FDG metabolism was found in other parts of the body; B, C. Nodular lesion in the right pulmonary artery wall, with an increased FDG uptake (SUVmax = 7.6); D. A radiological defect in the right pulmonary artery trunk is seen in the form of a striped hypodense lesion with a CT attenuation value of approximately 32 HU.

was -1.88, which were not consistent (**Figure 4G**). The patient underwent pulmonary artery endarterectomy after one week and the postoperative pathology showed round and spindle-shaped undifferentiated sarcoma cells and mucinous-like interstitium with obvious tumor cell anisotropy and localized necrosis (**Figure 5A**). Immunohistochemical staining showed CK (partial +), EMA (-), CD34 (-), ERG (-), CD31 (-), F8 (+/-), S-100 (-), NF (-), SMA (+), Desmin (+), SOX-10 (-), CD68 (partial +), Caldesmon (-), HMB45 (-) Melan-A (-), P53 (+), CD117 (-), DOG-1 (-), SYN (-), CD56 (+), H3K27me3 (+), Ki-67 (40% +) (**Figure 5B-I**). These findings were consistent with the diagnosis of PAS with smooth muscle sarcoma differentiation. After 2 cycles of postoperative treatment with "dacarbazine + carboplatin", the patient underwent PET/CT again, which showed a diffusely increased radioactive accumulation of soft tissue lesions around the ascending aorta walls, aortic arch and right pulmonary artery trunk (SUVmax = 8.2), considering postoperative inflammatory changes. A soft tissue nodule with increased FDG uptake in the left upper lobe lung near the hilum (SUVmax = 6.1) was found with the size at about 1.1 cm × 1.3 cm, suggesting metastasis. Besides, a radiological defect in the main trunk of the right pulmonary artery presenting with a hypodense lesion showed no change from previous examination (**Figure 6**). The patient is currently being treated with "etoposide + isocyclophosphamide + methotrexate" and is still being followed up.

Discussion

PAS is a malignant tumor arising from the pulmonary artery or pulmonary valve and in rare cases, which may spread retrogradely through the pulmonary valve to the right ventricular outflow tract. Clinical manifestations include dyspnea, chest pain, blood in sputum and hemoptysis due to hemodynamic abnormalities caused by tumor obstruction of the pulmonary artery, cyanosis, jugular venous irritation and pestle finger when combined with right heart insufficiency [7, 8]. The patient had different levels of elevated D-dimer, fibrinogen, and B-type natriuretic peptide, which were considered to be related to PAS secondary to thrombotic and inflammatory changes. PAS has multiple pathological types, including undifferentiated sarcoma, smooth muscle sarcoma, malignant fibrous tissue sarcoma, fibrosarcoma, etc [9]. This case belongs to undifferentiated sarcoma.

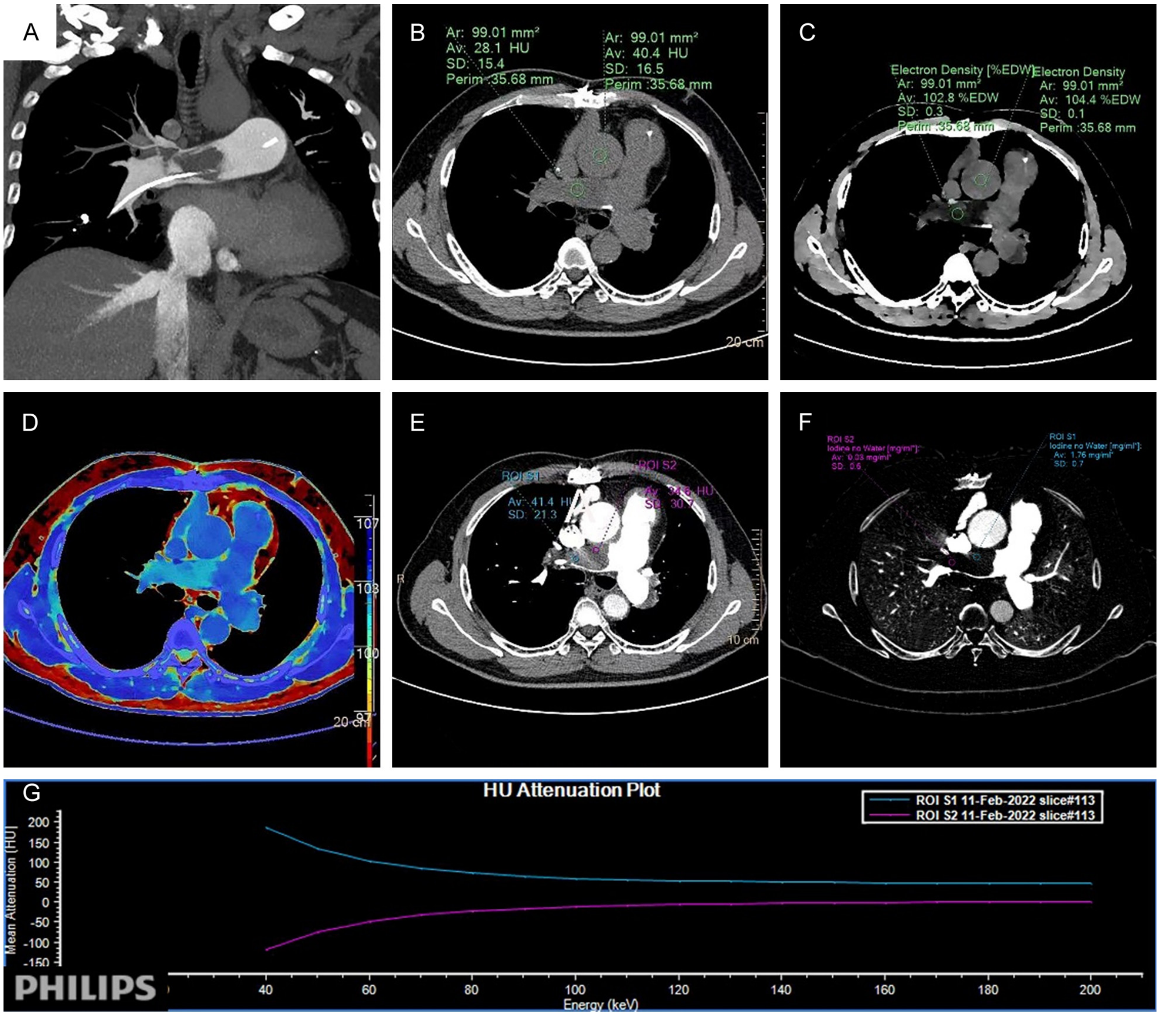

Figure 4. Spectral CT enhanced scan images. A. Arterial phase MIP images; B. The CT value of the ascending aorta was 40.4 HU and the CT attenuation value of the hypointense area in right pulmonary artery trunk was 28.1 HU on the plain scan mixed energy image; C. Electron density (ED) images showed an ED value of 104.4% EDW in the ascending aorta and an ED value of 102.8% EDW in the low electron density region of the right pulmonary artery trunk, with a non-uniform distribution in the low density region; D. The fused image of the hybrid energy image and ED image showed that the electron density region in the right pulmonary trunk had inhomogeneous low electron density, whereas the electron density of the ascending aorta and the rest of the pulmonary artery was uniform and the low electron density region is clearly differed from other regions; E. The mixed energy image showed a CT value of 41.4 HU in the S1 region and 34.6 HU in the S2 region; F. The contrast iodine density (ID) image displayed an ID value of 1.76 mg/ml in the nodal radioactive dense foci in **Figure 3B** and 0.03 mg/ml for the striped hypointense lesion in **Figure 3C**; G. The slope of spectral curve in the PAS region was 2.08 whereas that in the thrombus region was -1.88.

On CT images, the shape of PAS is mostly polypoid or nodular. Sometimes the outer wall of dilated vessels can be found to be heterogeneously altered, suggesting infiltration and dissemination by tumor lesions, while some lesions can directly invade adjacent tissues along the extravasation. The “wall-eclipsing sign” is considered to be the typical presentation of PAS, which refers to the invasion of one or both walls of the main pulmonary artery trunk [1, 10]. The mechanism of the “wall eclipsing sign” may be related to the origin of PAS in the intima or middle lamina of the pulmonary artery when the tumor gradually occupies the lumen of the pulmonary artery by internal subtle growth [11]. This case showed infiltrative growth of the attached wall on CT images, which is consistent with previous reports [11]. The CT manifestation of PAS is similar to that of PTE when both of them show filling defects and pulmonary artery dilatation in the pulmonary artery. However, PTE typically

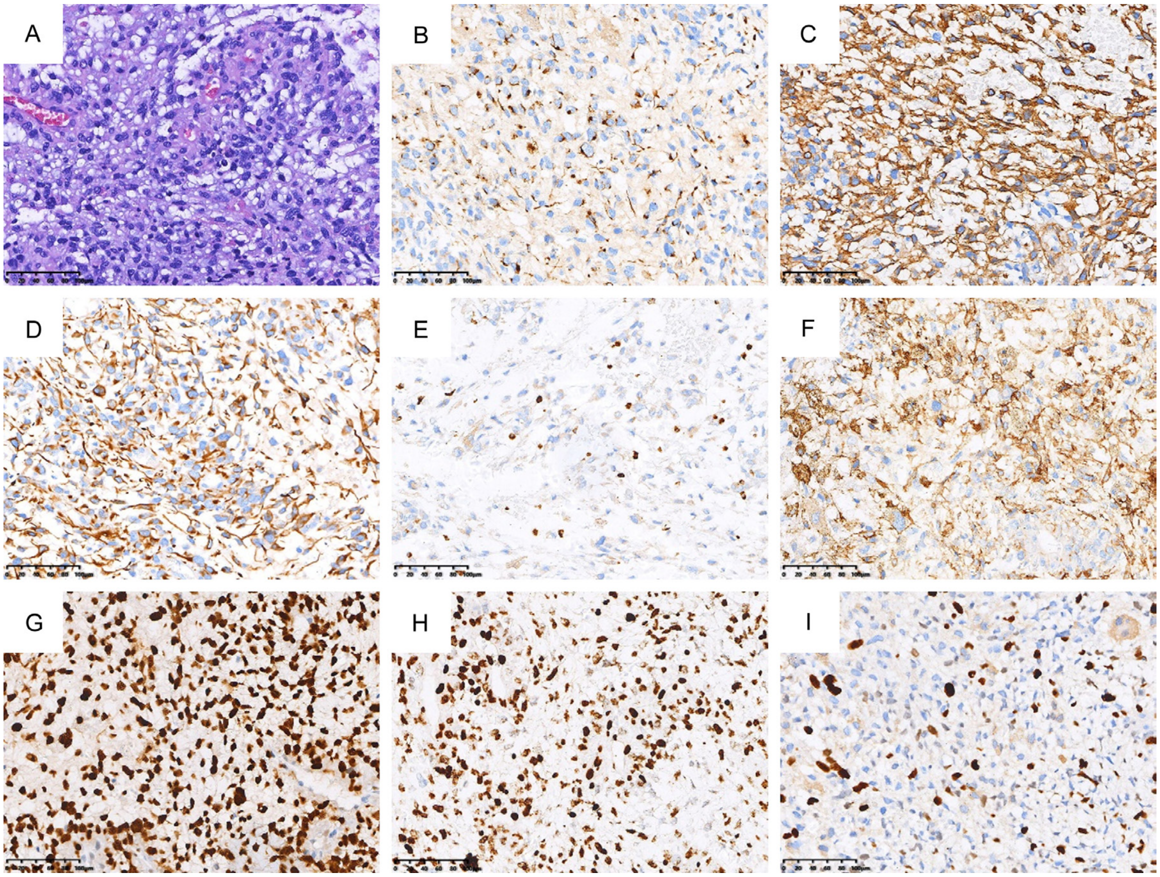

Figure 5. Histopathological images. (A) Hematoxylin-eosin (HE) staining (magnification × 200). Immunohistochemistry showed that the tumor cells were positive for CK (B), SMA (C), Desmin (D), CD68 (E), CD56 (F), P53 (G), H3K27me3 (H), and Ki-67 (I) [Envision (B-H) × 200].

has a history of deep vein thrombosis in lower extremities and the density of filling defects is more uniform. Furthermore, PTE lesions confined to the lumen of the vessel only without extra-luminal invasion so that the contact surface with blood flow is flatter than PAS, and the symptoms usually improve after anticoagulation.

Compared with conventional CT, dual-layer spectral computed tomography (DLCT) scan, as a new dual-energy examination modality, has more advantages in in lesion characterization and quantitative analysis, providing both anatomical information of lesions and quantitative data [12]. DLCT measures the X-ray attenuation at two different energies and evaluates the effective atomic number and electron density (ED) of each voxel, producing a more accurate electron density value and expressing as a percentage of electron density relative to water (%EDW) [13]. The spectral data can be reconstructed on Philips Workstation using the spectral-based imaging (SBI) data package to obtain conventional mixed energy images, effective atomic number images, contrast iodine density images, and electron density images. The electron density usually corresponds to the physical density of the tissue [14]. In this study, the patient's lesion measured 102.8% EDW on the ED, which was lower than that in the ascending aortic region (104.4% EDW), suggesting that the ED can be used to identify PAS with different physical densities from blood. Moreover, the fused image of hybrid energy image and ED can be formed on Philips Workstation, which improves the visualization of PAS diagnosis. Contrast iodine uptake by the tissue can be shown on iodine density (ID) images, providing the ID value of the selected region of interest [15]. The ID value of the arterial phase of PAS in this case (1.89 mg/ml) was significantly higher than that of the thrombus site (0.03 mg/ml) with different slope of the energy spectrum

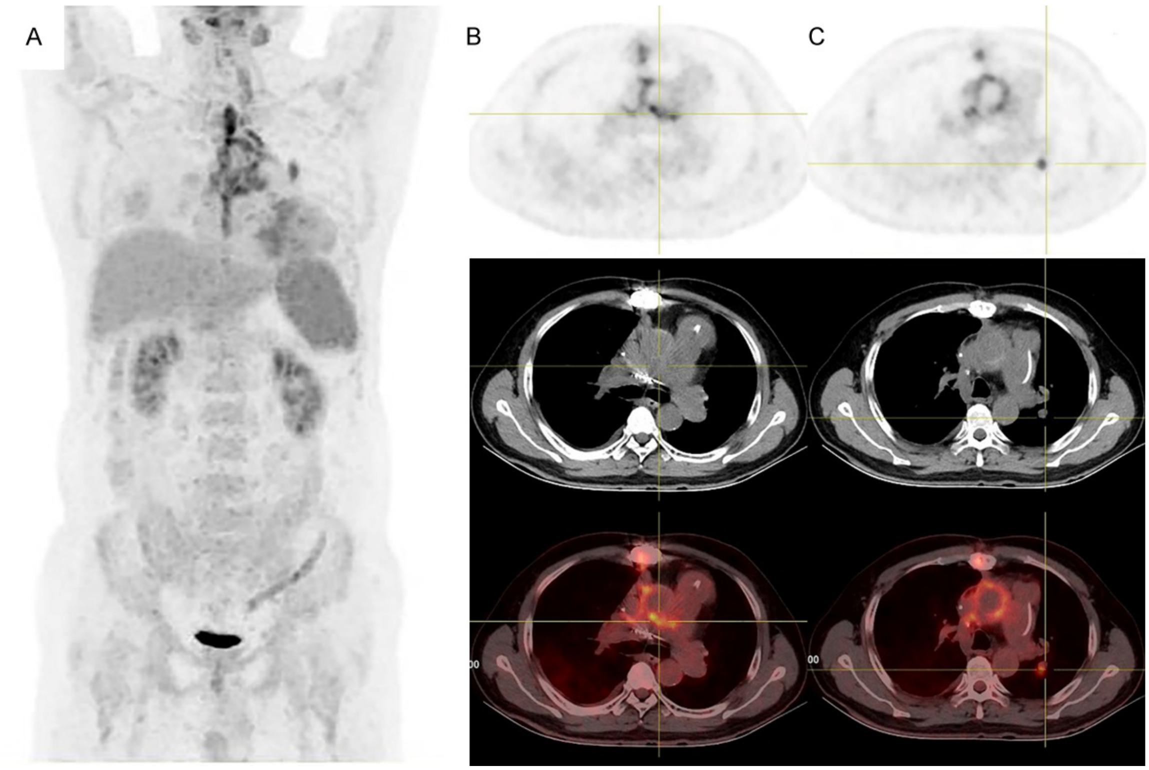

Figure 6. ^{18}F-FDG PET/CT images after the 2nd surgery. A. The MIP image demonstrated diffused hypermetabolic lesions around the ascending aorta, aortic arch, the main trunk of the right pulmonary artery, and the upper lobe of the left lung near the hilum; B. The transverse images demonstrated increased FDG uptake in the soft tissue (SUVmax = 8.2); C. The transverse images demonstrated a soft tissue nodule in the upper lobe of the left lung near the hilum with a higher FDG uptake (SUVmax = 6.1) at about 1.1 cm × 1.3 cm in size.

curve, which could also helpful to differentiate PAS from thrombus, reflecting the size of the lesion. ^{18}F-FDG PET/CT can comprehensively show the extent of lesions and metastases, effectively reduce mis-diagnoses, provide a basis for clinical staging and treatment plans, guide the clinical selection of biopsy sites, and improve the success rate and accuracy of biopsy. When PAS occurs pulmonary or mediastinal metastases, ^{18}F-FDG PET/CT can show the lesions with increased glucose metabolism which could be smaller than that in CT images [7, 10, 11]. The diagnosis of PAS could be considered when PET/CT imaging reveals nodular or striated hypermetabolic lesions along the pulmonary artery. Because thrombus uptake of FDG is rarely increased [16], the hypometabolism can easily exclude from the diagnosis of PTE. ^{18}F-FDG PET/CT was used by Tueller et al. [17] to diagnose PAS and provide initial staging, therefore, improving the outcome.

Surgical resection is the first-line treatment of PAS so that early diagnosis and radical surgical excision are vital to prolong the patient survival [1, 18]. Chemotherapy may provide some survival benefits, but still need to be proved. Despite surgical resection, ^{125}I-seeds implantation and multiple adjuvant chemotherapies can also be used in the patients with recurrence and metastasis. There are some limitations in this case report, such as the ongoing follow up and the lack of ultimate survival prediction.

Conclusion

In conclusion, PAS is clinically rare with atypical symptoms and should be considered in the differential diagnosis of pulmonary artery endarterectomy sarcoma when enhanced CT or pulmonary angiography shows a filling defect. Spectral CT and PET/CT show important roles in the evaluation of the lesion and metastases, providing a strong imaging basis for differentiating the diagnosis of pulmonary artery sarcoma from pulmonary embolism. Furthermore, PET/CT can also allow the treatment monitoring and follow-up.

Acknowledgements

This study was funded by the Beijing Science Foundation for Distinguished Young Scholars (JQ21025), the Peking University Medicine Fund of Fostering Young Scholars' Scientific & Technological Innovation (BMU2022PY006).

Disclosure of conflict of interest

None.

Address correspondence to: Dr. Lei Kang, Department of Nuclear Medicine, Peking University First Hospital, Beijing 100034, PR China. Tel: +86-(10)-83575252; E-mail: kanglei@bjmu.edu.cn

References

[1] Kronzer E, Robinson SI, Collins DA and McBane RD 2nd. Primary pulmonary artery sarcoma versus pulmonary thromboembolism: a multimodal imaging comparison. J Thromb Thrombolysis 2021; 52: 1129-1132.
[2] Jeong N, Seol SH, Kim IH and Kim JY. Pulmonary artery sarcoma - multimodality imaging. J Clin Imaging Sci 2016; 6: 45.
[3] Zhao M, Nie P, Guo Y and Chen H. Pulmonary artery intimal sarcoma: a rare cause of filling defects in pulmonary arteries. Am J Med Sci 2022: S0002-9629(22)00230-0.
[4] Hong YJ, Shim J, Lee SM, Im DJ and Hur J. Dual-energy CT for pulmonary embolism: current and evolving clinical applications. Korean J Radiol 2021; 22: 1555-1568.
[5] Pan B, Wang SC, Chen ZK and Chen X. Primary pulmonary artery sarcoma with intrapulmonary metastases based on PET/CT imaging: a case report and literature review. Ann Palliat Med 2021; 10: 7013-7018.
[6] Liu X, Hou J, Wang X and Chen Z. An intimal sarcoma of pulmonary artery mimicking pulmonary embolism: a case report and literature review. Respirol Case Rep 2017; 5: e00248.
[7] Pan B, Wang SC, Chen ZK and Chen X. Primary pulmonary artery sarcoma with intrapulmonary metastases based on PET/CT imaging: a case report and literature review. Ann Palliat Med 2021; 10: 7013-7018.
[8] Halank M, Jakob C, Kolditz M, Hoeffken G, Kappert U, Ehninger G and Weise M. Intimal pulmonary artery sarcoma presenting as severe dyspnea and right heart insufficiency. Onkologie 2010; 33: 313-316.
[9] Chahal A, Manapragada PP, Singh SP, Winokur TS and Sonavane SK. Primary intrathoracic sarcomas: a review of cross-sectional imaging and pathology. J Comput Assist Tomogr 2020; 44: 821-832.
[10] Gan HL, Zhang JQ, Huang XY and Yu W. The wall eclipsing sign on pulmonary artery computed tomography angiography is pathognomonic for pulmonary artery sarcoma. PLoS One 2013; 8: e83200.
[11] Wyler von Ballmoos MC, Chan EY and Reardon MJ. Imaging and surgical treatment of primary pulmonary artery sarcoma. Int J Cardiovasc Imaging 2019; 35: 1429-1433.
[12] Tivnan M, Wang W and Stayman JW. A prototype spatial-spectral CT system for material decomposition with energy-integrating detectors. Med Phys 2021; 48: 6401-6411.
[13] Hua CH, Shapira N, Merchant TE, Klahr P and Yagil Y. Accuracy of electron density, effective atomic number, and iodine concentration determination with a dual-layer dual-energy computed tomography system. Med Phys 2018; 45: 2486-2497.
[14] Bae K and Jeon KN. Diagnosis of pulmonary embolism in unenhanced dual energy CT using an electron density image. Diagnostics (Basel) 2021; 11: 1841.
[15] Celtikci P, Hekimoglu K, Kahraman G, Bozbas S, Gultekin B and Akay HT. Diagnostic impact of quantitative dual-energy computed tomography perfusion imaging for the assessment of subsegmental pulmonary embolism. J Comput Assist Tomogr 2021; 45: 151-156.
[16] Hmelik S, Dobrenić M and Huić D. F-18 FDG PET/CT in pulmonary artery sarcoma: clinical vignette. Nucl Med Rev Cent East Eur 2018; 21: 48-49.
[17] Tueller C, Fischer Biner R, Minder S, Gugger M, Stoupis C, Krause TM, Carrel TP, Schmid RA, Vock P and Nicod LP. FDG-PET in diagnostic work-up of pulmonary artery sarcomas. Eur Respir J 2010; 35: 444-6.
[18] Bandyopadhyay D, Panchabhai TS, Bajaj NS, Patil PD and Bunte MC. Primary pulmonary artery sarcoma: a close associate of pulmonary embolism-20-year observational analysis. J Thorac Dis 2016; 8: 2592-2601.